AIAA Modeling and Simulation Technologies Conference
2 - 5 August 2010, Toronto, Ontario Canada

AIAA 2010-7914

Modeling Human Dynamics in Combined Ramp-Following and Disturbance-Rejection Tasks

D.M. Pool,* M.M. van Paassen,† and M. Mulder‡
Delft University of Technology, Delft, The Netherlands

This paper investigates the modeling of human manual control behavior for pursuit tracking tasks in which target forcing functions consisting of multiple ramp-like changes in target attitude are used. Due to the use of a pursuit display and the predictability of such forcing function signals, it can be anticipated that a pursuit or precognitive control strategy, consisting of open-loop feedforward control inputs in response to the predictable reference signal, is applied by the human operator. If combined with an additional disturbance on the controlled element, a control task results that is similar to performing a commanded turn entry/exit or altitude capture in turbulence. It is as of yet uncertain if such pursuit or precognitive control is indeed used during such a control task, and to what extent a quasi-random disturbance would suppress pursuit/precognitive control strategies. A human-in-the-loop evaluation of the combined ramp-following and disturbance-rejection task was performed to gather data for the modeling of human manual control behavior. It is found that despite the anticipated pursuit and precognitive control inputs, classical compensatory models of human manual control dynamics are highly capable of describing human dynamics for these specific control tasks. Measured control inputs, however, are found to correspond well with proposed models for open-loop feedforward operations as well, suggesting future evaluation of a model of human behavior that combines, or switches between, error-reducing compensatory and open-loop feedforward operations.

I. Introduction

The theory of Successive Organization of Perception (SOP) put forth by McRuer et al.[1] defines three different levels of manual control behavior that can be adopted during manual tracking. Depending on defining features of the control task such as display format and tracking forcing function, human operators may revert to compensatory, pursuit, or precognitive control strategies, or could be switching between any combination of those. Most research into human manual control behavior has focused on purely compensatory control, typically for control tasks where tracking errors induced by a quasi-random forcing function signal are attenuated from a visual display. Considerable success has also been achieved in modeling of human manual control in both single-loop[2] and multimodal compensatory control tasks.[3–5] Despite the fact that most real-life manual control tasks induce pursuit or precognitive control strategies,[1] modeling of these higher levels of manual control behavior has received significantly less attention.

This paper focuses on manual control behavior in manual control tasks where a deterministic reference trajectory, defined as a number of discrete ramp-like changes in target attitude, is to be tracked using a pursuit display. In addition, a quasi-random disturbance signal is applied to perturb the controlled element dynamics. Compared to the control tasks that are typically used for studying the effects of physical motion feedback during manual control, where two quasi-random forcing function signals are applied,[3,5,6] such ramp target signals yield more realistic manual control tasks, similar to in-flight maneuvers such as a turn entry or altitude change in turbulence.[7,8] Furthermore, Ref. 9 has shown that, depending on ramp signal design, reliable identification of the multimodal pilot models that are used for modeling manual control under such multimodality conditions is possible using measurements taken during combined ramp-following and disturbance-rejection tasks.

For repetitive manual tracking of such deterministic ramp-like reference signals, however, it is likely that human operators will develop such familiarity with the reference signal and controlled element dynamics that it allows for

*PhD Candidate, Control and Simulation Division, Faculty of Aerospace Engineering, P.O. Box 5058, 2600GB Delft, The Netherlands; d.m.pool@tudelft.nl. Member AIAA.

†Associate Professor, Control and Simulation Division, Faculty of Aerospace Engineering, P.O. Box 5058, 2600GB Delft, The Netherlands; m.m.vanpaassen@tudelft.nl. Member AIAA.

‡Professor, Control and Simulation Division, Faculty of Aerospace Engineering, P.O. Box 5058, 2600GB Delft, The Netherlands; m.mulder@tudelft.nl. Member AIAA.

generation of open-loop precognitive control inputs.[1,10,11] In addition, despite the fact that the use of a pursuit display does not preclude the adoption of pursuit behavior by a human operator,[12,13] a pursuit display in combination with ramp signals with a predictable rate of change does provide ample opportunity for pursuit tracking. On the other hand, previous experimental work has hinted at suppression of pursuit operation when an additional disturbance signal is present,[14] as disturbances on the controlled element can only be attenuated using compensatory control.

It is the purpose of this paper to evaluate which mode of operation (or combination of modes) human controllers select for combined ramp-following and disturbance-rejection tasks. Due to the adaptivity of human control behavior it is likely that the type of control behavior (compensatory, pursuit, precognitive) that is adopted in such control tasks is dependent on both the characteristics of the ramp signals (steepness, magnitude) and the controlled element dynamics. This paper describes an experiment in which single-loop manual control behavior is evaluated for control of both single and double integrator dynamics. Note that the effects of physical motion feedback on manual control are not considered in this study. Rather, the focus lies on the human dynamics that occur during ramp-following, to which the effects of additional motion feedback are expected to be added in later work. Due to a likely effect of ramp signal design on control strategies and the modeling thereof, target signals with two different ramp steepnesses are considered, which are the same as those evaluated in Ref. 9. Using this experimental data, required extensions to the compensatory pilot models that are used in previous work[7–9,15] will be pointed out.

This paper is structured as follows. First, Sec. II provides a detailed description of the manual control task and gives an overview of the the pertinent literature on modeling manual control behavior for such a control task. Then, Sec. III describes the details of the human-in-the-loop experiment that was performed to gather the required measurements of human manual control behavior. The results of this experiment are presented in Sec. IV. The paper ends with a discussion and conclusions.

II. Background

II.A. Control Task

This paper investigates human manual control behavior in pitch-attitude tracking tasks performed with a pursuit display. Fig. 1 depicts a schematic representation of such a manual control task, where a human pilot controls the pitch attitude θ of the controlled element Y_c. Two forcing function signals are indicated in Fig. 1: the target forcing function f_t defines the reference trajectory that θ should follow as closely as possible, while f_d represents an external disturbance that works on the controlled element. Note that due to the use of a pursuit display as depicted in Fig. 2, the human pilot can use information on the target signal f_t, the tracking error e, and the controlled element state θ to achieve a suitable control input u.

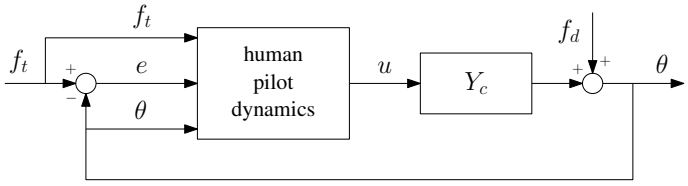

Figure 1. Schematic representation of a combined target-following and disturbance-rejection task.

Pursuit tracking tasks similar to the one depicted in Fig. 1 have been studied extensively in literature,[1,12,13,16] but mainly for control tasks with quasi-random target forcing function signals (f_t) and without further external disturbances (f_d). As a continuation of previous research,[7–9] this paper addresses human control behavior for tracking tasks in which the target signal is composed of a series of discrete ramp-like changes in reference attitude and an additional quasi-random disturbance signal is present. Fig. 3 depicts the two ramp target forcing functions (R1 and R10, which have different ramp steepnesses) and the quasi-random multisine disturbance signal (MS). The details of these forcing function signals are provided in Sec. III.

Human dynamics during manual control have been shown to be highly adaptable to the dynamics of the controlled element Y_c.[1,2] Therefore, this paper will investigate control behavior in the combined ramp-following and disturbance-rejection task defined by the forcing function signals depicted in Fig. 3 for both single and double integrator controlled element dynamics, given by:

$$Y_c(s) = \frac{K_c}{s}, \quad Y_c(s) = \frac{K_c}{s^2} \tag{1}$$

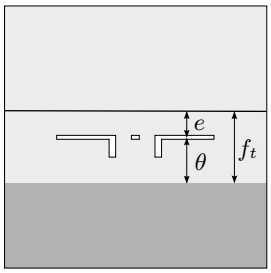

Figure 2. Pursuit display.

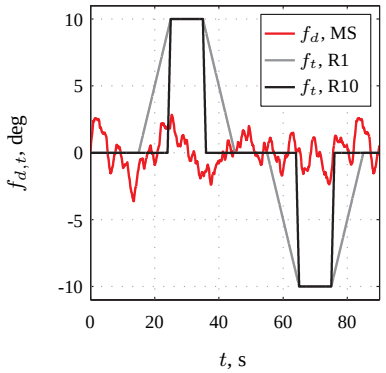

Figure 3. Time traces of the multisine disturbance forcing function (MS) and both ramp target forcing function signals (R1 and R10).

II.B. Successive Organization of Perception

In the 1960s, McRuer et al.[1] developed their theory of Successive Organization of Perception (SOP). This SOP theory defines three distinct levels of skill-based manual control behavior that can be adopted during manual tracking, depending on the nature and characteristics of the control task. Schematic representations of these three levels of manual control behavior are depicted in Fig. 4.

The lowest level of manual control behavior is referred to as compensatory behavior, which is depicted in Fig. 4(a). During compensatory control, the human operator only acts on the perceived tracking error e, thereby closing a single loop around the controlled element Y_c. Compensatory behavior is typically adopted during control tasks where tracking errors induced by a quasi-random forcing function signal are depicted on a compensatory display.[2]

If information other than the tracking error e is also available to the human operator, such as for instance provided on the pursuit display shown in Fig. 2, he may choose to utilize pursuit tracking behavior as depicted in Fig. 4(b). Even though the explicit presentation of f_t and θ on a pursuit display would allow the human operator to also operate on both those quantities, thereby utilizing a multi-loop control strategy, this is no guarantee for the utilization of a pursuit tracking strategy. As rightly pointed out by Hess,[13] a distinction needs to be made between external changes in available variables and the internal organization of the human operator's control strategy. This also implies, as argued by McRuer et al.,[1] that higher level control behavior might occur for purely compensatory tracking tasks if, for instance, the forcing function signal is recognizably repetitive or predictable.

The final type of control behavior depicted in Fig. 4 is precognitive control. Such control behavior typically occurs in control tasks where certain stored control commands are to be given in response to a trigger (see Fig. 4(c)). Predictable forcing function signals as considered in this paper (see Fig. 3) are an example of an control task that, given extensive training and familiarization, would support a precognitive control strategy.

The taxonomy of control behavior summarized in the SOP theory and Fig. 4 is a useful starting point for the evaluation of control behavior in the combined ramp-following and disturbance-rejection tasks studied in this paper. As can be verified from all three block diagrams depicted in Fig. 4, a disturbance signal on the controlled element output can only be attenuated through a (compensatory) feedback control strategy. To what extent the presence of such a disturbance signal clashes with the human dynamics required for following of ramp target signals is as of yet unknown. The same holds for the modeling of these human dynamics.

II.C. Modeling Manual Control Behavior

II.C.1. Modeling Compensatory Control

The modeling of compensatory control behavior as depicted in Fig. 4(a) has been well established since the work of McRuer et al.[2] Using measurements of pilot dynamics for a multitude of different controlled elements and forcing function signals, McRuer et al. developed a models and accompanying sets of rules of thumb that have proven to be widely applicable for describing compensatory pilot dynamics. Here, the following model, which is based on the work of McRuer et al.,[2] is used:

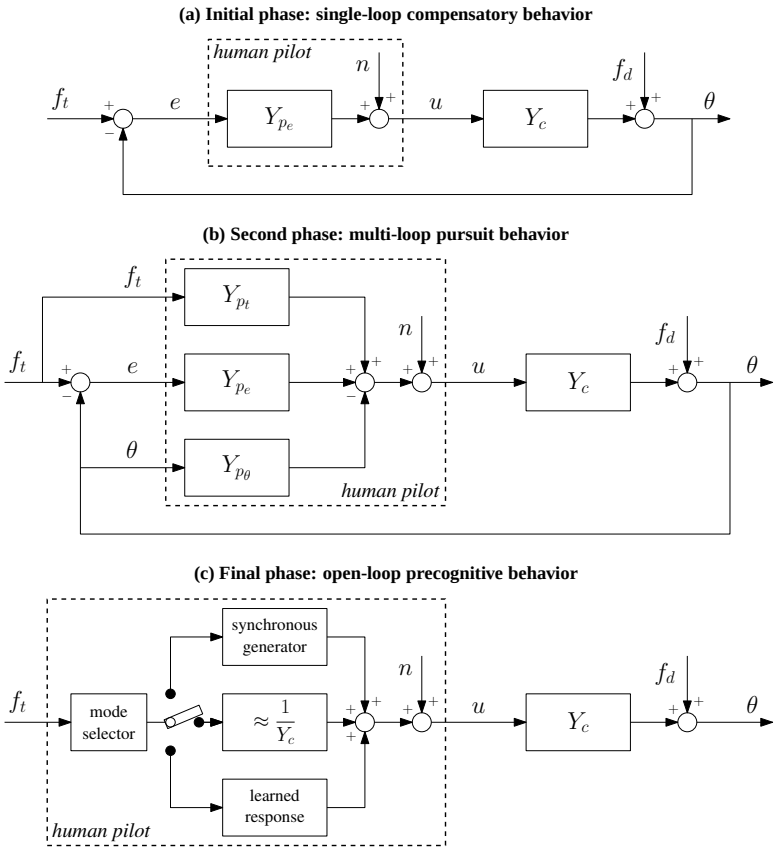

Figure 4. The different phases in the Successive Organization of Perception. Adapted from Ref. 1.

$$Y_{p_e}(s) = K_{p_e}\left(1 + sT_{L_e}\right) e^{-s\tau_e} Y_{nm}(s) \tag{2}$$

In Eq. (2), $K_{p_e}(1 + sT_{L_e})$ represents the pilot equalization characteristic. Note that in the original model as described in Ref. 2 this equalization characteristic was defined as a lead-lag transfer function. McRuer et al.,[2] however, established that human operators adapt their equalization characteristics to yield an open-loop system ($Y_{p_e}Y_c$) with approximately single integrator dynamics around gain-crossover.[2] This implies that for single integrator controlled element dynamics, the equalization characteristic as given in Eq. (2) is reduced to only the proportional gain K_{p_e}. For double integrator dynamics, low-frequency lead needs to be generated to achieve K/s dynamics around crossover. Therefore, the full equalization characteristic listed in Eq. (2) is needed for describing human dynamics during compensatory double integrator control. Note, however, that lag equalization is required for neither controlled elements. The delay parameter τ_e accounts for any delays internal to the pilot that accumulate in generating a compensatory control input. Finally, the transfer function Y_{nm} represents the combined dynamics of the neuromuscular actuation and the manipulator,[17] which are modeled as a second-order mass-spring-damper system:

$$Y_{nm}(s) = \frac{\omega_{nm}^2}{s^2 + 2\zeta_{nm}\omega_{nm}s + \omega_{nm}^2} \tag{3}$$

The neuromuscular frequency ω_{nm} and damping factor ζ_{nm} are free parameters of this compensatory model, as are K_{p_e}, τ_e, and T_{L_e} (the latter for double integrator control only).

II.C.2. Modeling Pursuit/Precognitive Control

Compared to the modeling of compensatory manual control behavior, the modeling of pursuit and precognitive tracking has received only moderate attention.[1,10,12,13,16] One of the reasons for this is the fact that during both pursuit tracking and control tasks where precognitive inputs are given, manual control behavior will involve responses to multiple perceived variables. This is, for instance, clear for a pursuit display configuration as presented in Fig. 2. This

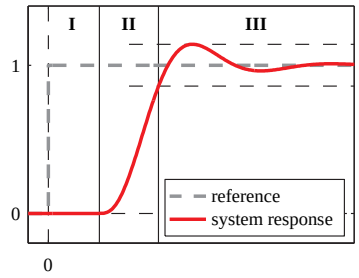

Figure 5. Hypothetical response of controlled element output during step tracking. Adapted from Ref. 1. I = Time delay phase, II = Rapid response phase (precognitive), III = Error reduction phase (compensatory).

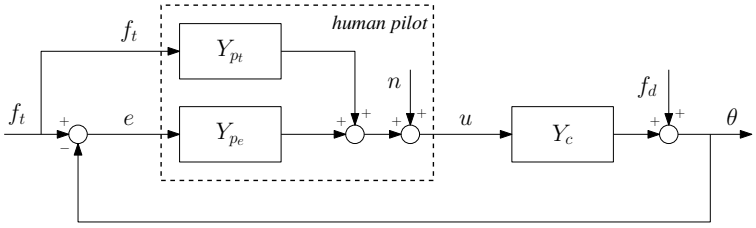

Figure 6. Two channel model of pursuit/precognitive control. Adapted from Ref. 1.

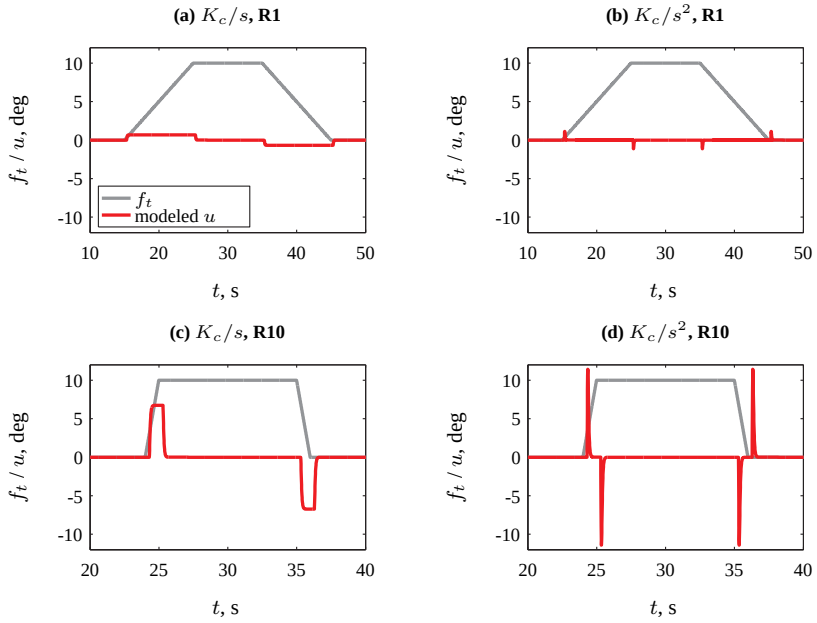

Figure 7. Example feedforward control inputs resulting from the proposed model of Eq. (4).

makes the modeling of such multimodal control behavior significantly more complex than the modeling of purely compensatory behavior.[12,13]

For pursuit tracking, Wasicko et al.[12] have shown that due to the fact that $e = f_t - \theta$, pursuit control behavior can be captured by considering only two of the three pilot responses depicted in Fig. 4(b), Y_{p_t}, Y_{p_e}, and Y_{p_θ}. Allen and McRuer[16] have therefore proposed to model pursuit control behavior with only the Y_{p_t} and Y_{p_e} channels depicted in Fig. 4(b), that is, as a closed-loop compensatory control strategy combined with feedforward control on the target signal.

For precognitive control inputs in a control task with predictable forcing function signals as considered here, the representation of Fig. 4(c) would only hold when the human operator's internal representation of f_t in Y_c allows for perfect execution of the appropriate control response. During actual manual control this can, however, be expected to never fully be the case. Hence, McRuer and Krendel[10] argue that compensatory error reduction will still be utilized after an initial precognitive control input is given, as illustrated by Fig. 5. Such a dual-mode representation of control behavior, where the human operator is hypothesized to switch between Y_{p_e} and Y_{p_t} upon a certain trigger, yields a control theoretic structure equal to that proposed by Allen and McRuer[16] for pursuit tracking, see Fig. 6.

For modeling of the compensatory response in the two-channel model of Fig. 6, some authors have suggested to use the form of Eq. (2),[1,12] thereby assuming similar compensatory human dynamics as encountered for pure compensatory control. As to the contents of the Y_{p_t} block of Fig. 6, it has been argued that for optimal performance of the feedforward Y_{p_t} should approximate the inverse of the controlled element dynamics, yielding $Y_{p_t} Y_c \approx 1$.[1,12,13]

From Fig. 6 it can be verified that if this is the case, θ will approximate f_t. As it can be anticipated that feedforward control will, however, not be perfect, this paper suggests the following model for the feedforward response Y_{p_t}:

$$Y_{p_t}(s) = K_{p_t} \frac{1}{Y_c(s)} Y_{eq_t}(s) e^{-s\tau_t} \tag{4}$$

In Eq. (4), K_{p_t} and τ_t are the gain an time delay associated with this feedforward response. These parameters are equivalent to K_{p_e} and τ_e in the compensatory model of Eq. (2). Further dynamics of Y_{p_t} are then governed by the inverse controlled element dynamics and the transfer function Y_{eq_t}, which represents further equalization performed by the operator on the target signal, analogous to the lead equalization in Eq. (2). Here it is proposed, as a starting point for further investigation, to set Y_{eq_t} to:

$$Y_{eq_t}(s) = \frac{1}{1 + sT_{I_t}} \tag{5}$$

This first-order lag is included in the model for Y_{p_t} to allow for capturing lags that may accumulate in this feedforward channel. These lags could result, for instance, from limitations on the inversion of Y_c by the human operator, or, as it is unlikely that human operators will attempt to precisely follow f_t, especially for steep changes in reference value, represent internal filtering or smoothing of the input. To visualize the responses the model of Eq. (4) is capable of describing, Fig. 7 shows theoretical control inputs for both ramp signals depicted in Fig. 3, and for both single and double integrator controlled elements. For generating the data shown in Fig. 7, the following parameter values have been used: $K_{p_t} = 1.0$, $\tau_t = 0.3$ sec, and $T_{I_t} = 0.05$ sec.

III. Experiment

III.A. Setup

III.A.1. Apparatus

To gather the data needed for testing the models proposed in Sec. II.C, an experiment was performed in the SIMONA Research Simulator (SRS) at Delft University of Technology, see Fig. 8. During the tracking tasks performed for this experiment, both the motion system and the outside visual system of the simulator were switched off. The (foveal) pursuit display (see Fig. 2) was projected on the primary flight display (PFD) in the SRS cockpit. The PFD update rate was 60 Hz and the time delay of the image generation on this PFD has been measured to be in the order of 20-25 ms (including the projection) using a custom visual delay measurement system.[18]

Participants used the pitch axis of an electrical sidestick to give their control inputs, u. The sidestick was calibrated to have no break-out force and a maximum deflection of ± 13 deg in pitch. Stick stiffness was set to 1.5 N/deg over the full range of pitch stick deflections. The roll axis of the sidestick was locked during the experiment.

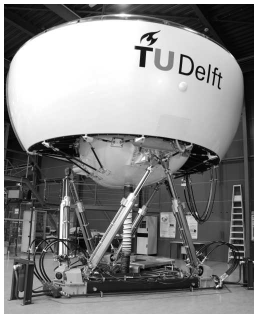

Figure 8. The SIMONA Research Simulator.

III.A.2. Controlled Element Dynamics

As already stated in Sec. II, the feedforward part of precognitive and pursuit control behavior is hypothesized to be proportional to the inverse of the controlled element dynamics, $Y_{p_t} Y_c \approx 1$.[1,12,13] For this reason, two different controlled elements were considered in this experiment: single (K_c/s) and double (K_c/s^2) integrator dynamics (Eq. (1)). The controlled element gain K_c was tuned to yield similarly optimal control authority with respect to the disturbance signal (see Fig. 3) for both controlled elements within the range of sidestick inputs (± 13 deg). For the single integrator dynamics K_c was set to 1.5, while for the double integrator K_c was taken equal to 8.0.

III.A.3. Forcing Functions

The target and disturbance forcing function signals that were applied in the experiment are depicted in Fig. 3. The ramp target signals, both consisting of one positive and one negative commanded pitch excursion, are the same as those considered in a previous theoretical investigation into multimodal pilot identification using such forcing function signals.[9] This previous work indicated improved identification results for such target signals with steeper ramps. In addition, as both pursuit and precognitive control are modeled with a response (Y_{p_t}) to which the target signal f_t is the

input, control inputs were also expected to change as a function of ramp signal steepness, as illustrated by Fig. 7. For these reasons, two levels of ramp steepness were considered in this experiment: 1.0 deg/s and 10.0 deg/s. Note that these two values of ramp steepness represent extreme values of those considered in Ref. 9, the former being relatively benign, the latter approximating a step input. These two ramp target forcing function signals are referred to in the following as R1 and R10, respectively.

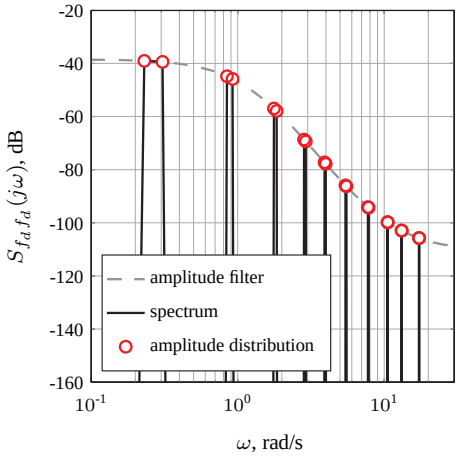

Figure 9. Quasi-random disturbance forcing function spectrum and amplitude distribution.

Table 1. Multisine disturbance forcing function data.

n_d	ω_d	A_d	ϕ_d
–	rad/s	deg	rad
3	0.2301	0.9588	1.9611
4	0.3068	0.9353	0.3818
11	0.8437	0.6855	5.4408
12	0.9204	0.6479	5.9008
23	1.7641	0.3415	6.1193
24	1.8408	0.3233	5.1898
37	2.8379	0.1739	5.5133
38	2.9146	0.1670	0.7492
51	3.9117	0.1058	3.3134
52	3.9884	0.1027	6.2120
71	5.4456	0.0643	1.9044
72	5.5223	0.0630	5.4372
101	7.7466	0.0402	1.2647
102	7.8233	0.0398	6.1412
137	10.5078	0.0291	5.0417
138	10.5845	0.0289	6.0918
171	13.1155	0.0243	2.2620
172	13.1922	0.0242	3.9989
225	17.2573	0.0206	5.2100
226	17.3340	0.0205	3.1755

The time trace of the multisine disturbance signal f_d, referred to as MS in the remainder of this paper, is also depicted in Fig. 3. This signal was generated as a sum of $N_d = 20$ sinusoids:

$$f_d(t) = \sum_{k=1}^{N_d} A_d(k) \sin\left[\omega_d(k)t + \phi_d(k)\right] = \sum_{k=1}^{N_d} A_d(k) \sin\left[n_d(k)\omega_m t + \phi_d(k)\right] \tag{6}$$

The sinusoid frequencies ω_d were chosen to cover the complete frequency range of interest for evaluation of pilot dynamics. To allow for measurement of frequency-domain pilot describing functions[6] and evaluation of coherence of pilot control with respect to the disturbance signal,[17] pairs of neighboring frequencies were selected that all fit an integer number of times (n_d) into the experimental measurement time T_m. All sinusoid frequencies were therefore integer multiples of the experimental measurement base frequency $\omega_m = 2\pi/T_m$. The experimental measurement time for this experiment was 81.92 seconds, yielding a base frequency of $\omega_m = 0.0767$ rad/s.

Sinusoid amplitudes A_d were defined according to the same low-pass filter amplitde distribution used in previous experiments.[17,19] Amplitudes were scaled to yield a disturbance signal with a time-domain variance of 1.5 deg^2. The spectrum of f_d, showing this low-pass distribution, is depicted in Fig. 9. The filter frequency response is depicted in gray, while the full spectrum of f_d is depicted in black. Red markers indicate the magnitudes of $S_{f_d f_d}$ equivalent to the selected sinusoid amplitudes A_d. The sinusoid phases ϕ_d were selected from a large number of randomly generated sets of phases to yield a disturbance signal with average maximum absolute excursion, rate and acceleration and an approximately normal distribution.[20] The numerical values for all disturbance forcing function parameters are listed in Table 1.

III.A.4. Independent Variables

Due to their hypothesized effect on manual control behavior for the control task depicted in Fig. 1, three different independent variables were varied in the experiment: the controlled element dynamics, the steepness of the ramps in the target forcing function signal, and the presence of the quasi-random disturbance signal. For both single and double

integrator controlled elements, the tracking task was performed in a baseline compensatory configuration where only f_d was present ($f_t = 0$). A further four conditions for each controlled element resulted from the factorial variation of ramp signal steepness (R1 and R10) and the presence of the disturbance signal (MS). This yielded a total number of ten experimental conditions, which are listed in Table 2.

Table 2. Experimental conditions.

Symbol	$Y_c(s)$	f_t	f_d
S1	$\frac{K_c}{s}$	–	MS
S2		R1	–
S3		R1	MS
S4		R10	–
S5		R10	MS
D1	$\frac{K_c}{s^2}$	–	MS
D2		R1	–
D3		R1	MS
D4		R10	–
D5		R10	MS

Table 3. Experiment Latin square design.

subject	session I					session II				
1	S5	S1	S2	S3	S4	D5	D3	D4	D2	D1
2	D1	D4	D5	D3	D2	S3	S4	S5	S1	S2
3	S1	S2	S3	S4	S5	D4	D2	D3	D1	D5
4	D2	D5	D1	D4	D3	S2	S3	S4	S5	S1
5	S4	S5	S1	S2	S3	D3	D1	D2	D5	D4
6	D1	D4	D3	D2	D5	S1	S2	S4	S3	S5

In the following, these different experimental conditions – that is, combinations of Y_c, f_t, and f_d – will be referred to using the symbols listed in Table 2. For instance, the pure compensatory conditions for single and double integrator controlled elements are indicated by S1 and D1, respectively.

III.A.5. Participants, Experimental Procedures, and Instructions

Six subjects were asked to perform the tracking task for the ten experimental conditions listed in Table 2. All participants were students or staff of the Faculty of Aerospace Engineering and all had extensive experience with manual tracking tasks from previous human-in-the-loop experiments. All participants were male, and their ages ranged from 25 to 47 years old.

As indicated in Table 3, all subjects performed the experiment in two separate sessions, which were both completed in the same week. Each session consisted of all variations in target and disturbance forcing function settings (see Table 2) for one of the controlled elements. For both controlled elements, the different forcing function conditions were randomized over the different subjects according to a balanced Latin square design. In addition, half of the participants first performed the single integrator control task in the first session (gray shaded cells in Table 3), while the other half first performed the double integrator control tasks.

The individual tracking runs of the experiment lasted 90 seconds, of which the last 81.92 seconds were used as the measurement data. For each experimental condition, participants' tracking performance was monitored by the experimenter. When participants had clearly reached a stable operating point and their proficiency in performing the tracking task had reached an asymptote, five repetitions at this constant level of tracking performance were collected as the measurement data. Typically, two short breaks (max. 30 minutes) were taken during each session, always after finishing the measurements for one condition and before starting the next. On average, each session took 2.5–3 hours to complete.

Participants were instructed to continuously attempt to minimize the pitch tracking error e presented on the visual displays, by minimizing the deviation of the target line with respect to the aircraft symbol (see Fig. 2). After each run subjects were informed of their tracking score, defined by the root mean square (RMS) of the error signal e, in order to motivate them to constantly control at their maximum level of performance.

III.A.6. Dependent Measures

During the experiment, the time traces of the error signal e, the control signal u, and the pitch attitude θ were recorded for each measurement run. From these measured time traces, several dependent measures are calculated to give insight into the effects of the independent variables manipulated during the experiment on manual control behavior. First, tracking performance and control activity – expressed as the time-domain variance (σ^2) of the error and control signals, respectively – are evaluated briefly for comparison with compensatory measurements from previous work.[2] In addition, σ_e^2 and σ_u^2 are analyzed to reveal the effects of the ramp forcing function signals on performance and control activity.

The main dependent measures considered in this paper, however, are those related to the models of manual control behavior introduced in Sec. II.C. Both the compensatory (Y_{p_e}) and feedforward (Y_{p_t}) models proposed in this section have been fit to the measured time traces using time-domain identification methods.[21] Note that a full combined model, as depicted in Fig. 6, is not yet evaluated in this paper. In addition to the identified model parameters, the extent to which the identified models can describe measured control inputs u is evaluated. For this, the variance accounted for (VAF) of the modeled control signal $\hat{u}$ is defined as:

$$\text{VAF} = \left[1 - \frac{\sum_{i=1}^{N} |u^2(i) - \hat{u}^2(i)|}{\sum_{i=1}^{N} u^2(i)}\right] \times 100\% \tag{7}$$

This VAF defines the percentage of the measured control signal u that is explained by the model. In this paper it will be used to evaluate how well the different models of manual control behavior describe the collected measurements.

III.B. Hypotheses

It is anticipated that due to the repetitive tracking of deterministic target input signals, some evidence of human operations on the target signal, perhaps in addition to compensatory operations on the tracking error e, can be found from behavioral measurements. Especially for the conditions without the quasi-random disturbance signal (S2, S4, D2, and D4), the combination of the pursuit display and the predictable target signals is expected to allow for a control strategy in which Y_{p_t} is dominant.

Furthermore, it is expected that the presence of the quasi-random disturbance signal might put more emphasis on the compensatory control loop the human operator needs to close, thereby suppressing open-loop feedforward control in favor of a more stable closed-loop. This would suggest tracking performance and compensatory pilot model parameters for conditions S3/S5 and D3/D5 are anticipated to be similar to those found for the pure compensatory conditions S1 and D1, respectively. Due to the less prominent effect on task performance, this effect is expected to be largest for the lowest steepness ramp signal (R1).

IV. Results

IV.A. Measured Time Traces

Fig. 10 presents sample time traces of the tracking error, control input, and pitch attitude recorded during the experiment for subject 1 in control of single integrator dynamics. Each row of graphs depicts these three signals for each of the five variations in forcing function settings (see Table 2). Each graph depicts the forcing function signal (for the graphs of e and u scaled down for plotting purposes) in gray and the five collected measurements of the depicted variable in black. The time-domain average of these five recordings is depicted in red, to show the consistency in the measurements. Note that for each set of time traces, the graphs for the different experimental conditions have the same y-axis scaling, to allow for quantitative comparison. Furthermore, note that only 40 seconds of the total run length (90 seconds) are depicted here.

First of all, Fig. 10 clearly shows the effect of the disturbance signal on the recorded signals. Where for the conditions where f_d is not present (S2 and S4) the depicted signals only show activity around the interval where a ramp in f_t occurs, the disturbance signal continuously induces tracking errors and hence control inputs. Furthermore, Fig. 10 also clearly shows an effect of ramp signal steepness. Figures Fig. 10(j) and (m) clearly show significant build-up of the tracking error directly after the occurrence of a R10 ramp due to the delay in the operator's response, as illustrated by Fig. 5. As can be verified from Figures Fig. 10(d) and (g), the effect of the R1 ramps on the tracking error is of significantly lower magnitude. The corresponding graphs of the control signal u show the same effect of ramp signal steepness. Especially for the conditions where the disturbance is present (S3 and S5), the control inputs that are performed in response to the target signal clearly stand out from those needed to attenuate the disturbance for condition S5, while they appear to be lost in the compensatory control action for S3. Finally, note from the time traces of the pitch attitude θ that overshoots in the following of the ramp signals are typically markedly larger for the steeper ramps (S4 and S5) than for R1 (S2 and S3).

IV.B. Tracking Performance and Control Activity

Highly similar measurements to those depicted in Fig. 10 were also obtained for the double integrator dynamics and for the other participants in the experiment. To evaluate the average effect of the independent variables of the experiment

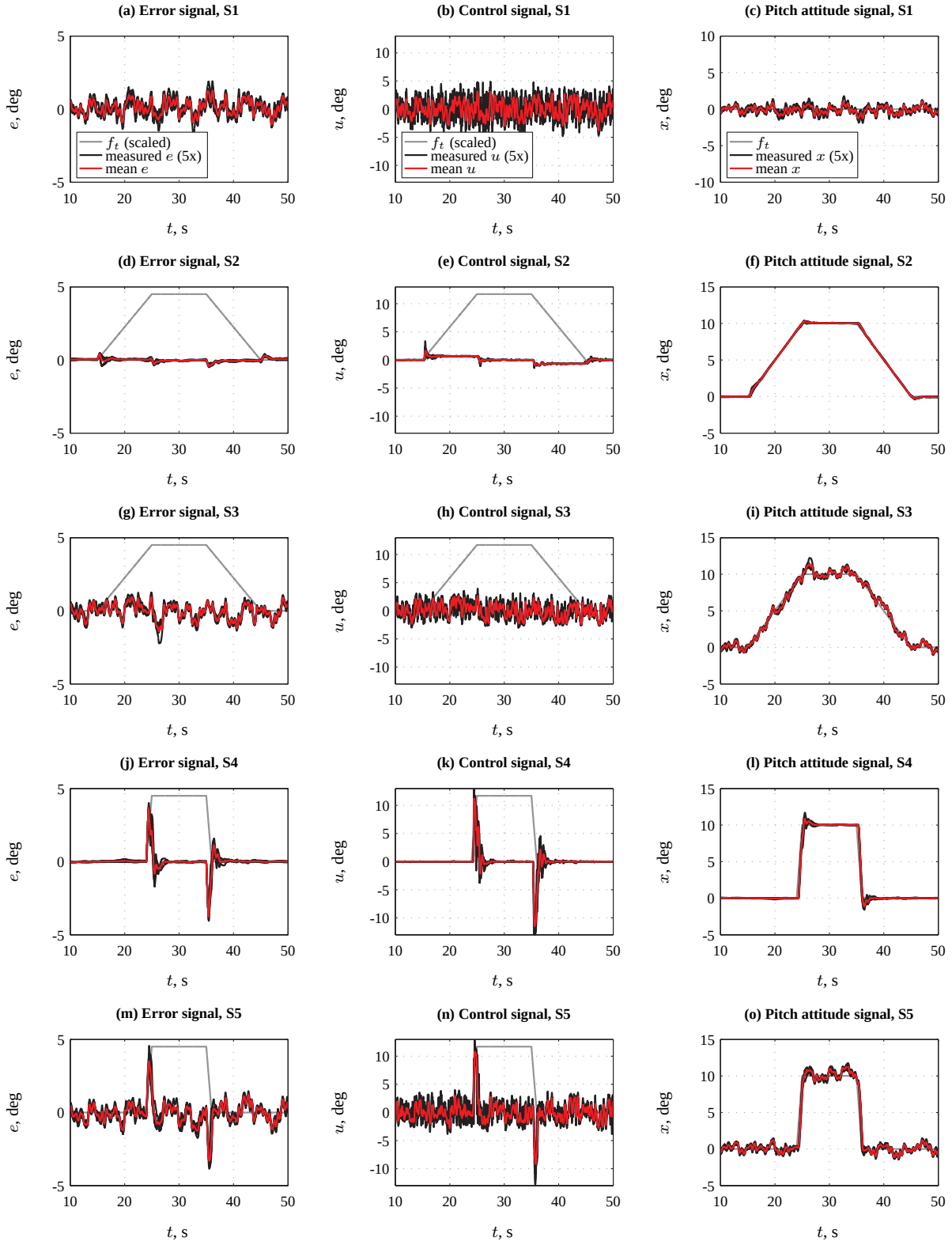

Figure 10. Measured time traces of e, u, and θ for control of single integrator dynamics (conditions S1-S5, subject 1).

on the tracking error and control input signals, Fig. 11 depicts the means of the tracking error and control input variance (σ_e^2 and σ_u^2, respectively) taken over the six experiment participants. The variance bars indicate the corresponding 95% confidence intervals. The depicted data has been corrected for between-subject variance.

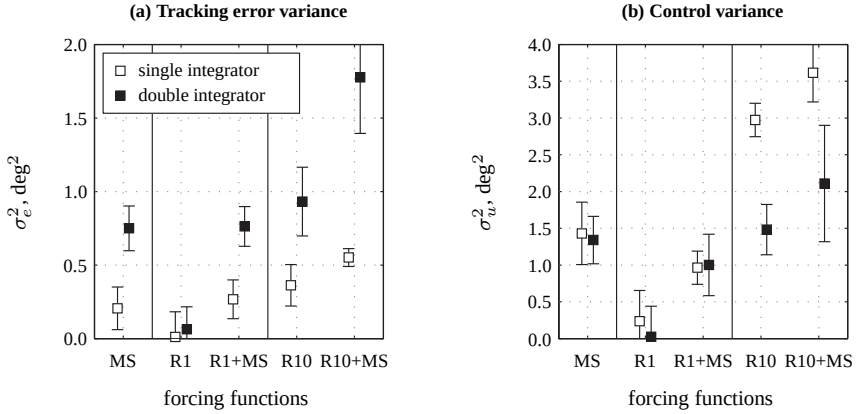

Figure 11. Average tracking performance and control activity.

Fig. 11(a) clearly shows tracking performance was found to be consistently worse (higher σ_e^2) for the double integrator controlled element. This is an expected result based on previous work,[2] due to the fact that double integrator dynamics are significantly more difficult to control than integrator dynamics. Note from Fig. 11(a) that this is somewhat independent of the applied forcing function signals.

Furthermore, Fig. 11(a) also shows that tracking errors for conditions S2 and D2, where only the R1 ramp signal was present, are very small compared to those for the other conditions. This shows that participants were able to keep tracking errors during the following of this low-steepness ramp signal very small, as can also be verified from Fig. 10. For the steeper ramp signal (conditions S4 and D4) tracking errors were found to be markedly larger. This can be attributed to more rapid build-up of tracking error for these steeper ramps, which already yield significant tracking errors within in the human operator's reaction time (see Fig. 10). Overall, especially for the single integrator data, the addition of the disturbance signal during ramp tracking is seen to increase tracking error variance by approximately the error variance found for the MS conditions. Note from Fig. 11(a) that this implies almost equal tracking performance for the MS and R1+MS conditions for both controlled elements.

Fig. 11(b) depicts the measured control signal variance for all conditions of the experiment. Note that control activity for the condition with only the disturbance signal (MS) is found to be almost equal for the single and double integrator controlled elements. This confirms the selection of appropriate values for the controlled element gain K_c as described in Sec. III.A.2. Fig. 11(b) further shows very low control activity for both controlled elements for the conditions with only the R1 target, as also expected from Fig. 7. Surprisingly, control activity is found to be slightly lower for the control tasks with both the R1 target and the disturbance signal (R1+MS) than for the corresponding conditions with only the disturbance signal (MS). For tracking of the steeper ramp signal, consistently higher control activity is found, which would be expected from the clear peaks during ramp tracking depicted in Fig. 10. In addition, control activity is found to be markedly higher for the single integrator than for the double integrator data.

IV.C. Modeling Behavior for Pure Disturbance-Rejection Tasks

For the conditions where no ramp target signal was present, but only the effects of the quasi-random disturbance signal were to be attenuated (that is, S1 and D1), a compensatory control task equivalent to those considered by McRuer et al.[2] is obtained. Therefore, pilot control behavior for these conditions can be described with the compensatory pilot model described in Sec. II.C.1. Fig. 12 depicts the frequency responses of the fits of Eq. (2) to data from conditions S1 and D2 for subject 1. In addition to the model fit shown in red, Fig. 12 also depicts the describing function estimate, calculated at the frequencies of f_d.[6]

Fig. 12 shows that the estimated describing functions, which are independent of the selected pilot model, correspond well with the frequency responses of the fitted compensatory behavior model. In addition, note that the VAFs of the depicted pilot models for conditions S1 and D1 are 75 and 85%, respectively, indicating that the remnant n is confirmed to contribute a typical 20-25% to the variance of the control signal u.[21]

Furthermore, note the marked difference between the compensatory control of single and double integrator dynamics, as expected based on the work of McRuer et al.[2] As can be verified from Fig. 12(a) and (c) human dynamics are

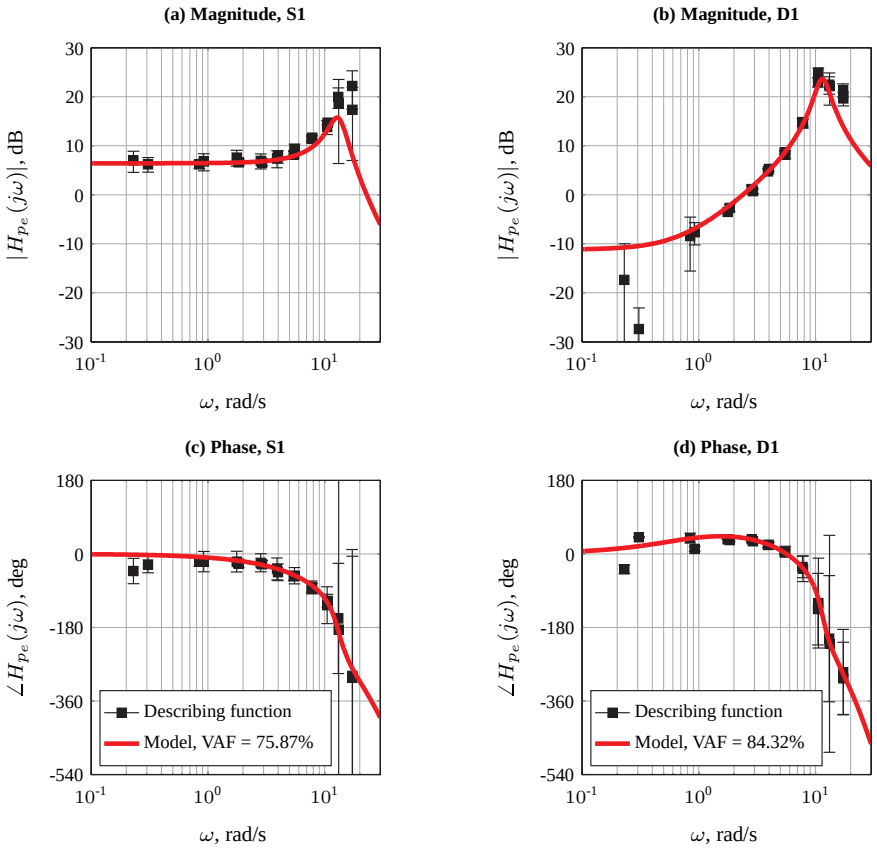

Figure 12. Example pilot describing functions and compensatory model fits for compensatory conditions (S1 and D1, subject 1).

approximately those of a pure gain, with the peak attributed to the combined neuromuscular and manipulator dynamics[17] just above 10 rad/s. In comparison, Fig. 12(b) and (d) (condition D1) show control behavior where significant phase lead is generated by the human operator, to compensate for the controlled double integrator dynamics.[2]

Highly similar model fits to those shown in Fig. 12 were obtained for the other participants in the experiment. Table 4 presents the average estimated compensatory model parameters for conditions S1 and D1, in addition to the average VAF of the model fit. The final column of Table 4 indicates an average model VAF of 85% for both the S1 and D1 conditions, indicating accurate compensatory model fits. Furthermore, the estimated parameter values listed in Table 4 reflect the different control behavior shown in Fig. 12. On average participants were generating low-frequency lead for frequencies above 0.75 rad/s for condition D1, at the cost of a marked increase in the compensatory time delay τ_e. These results are highly consisted with those reported in Ref. 2 and later publications on compensatory manual control.

Table 4. Average compensatory parameters and model VAF for conditions S1 and D1.

Condition	K_{p_e}	T_{L_e}, s	τ_e, s	ω_{nm}, rad/s	ζ_{nm}	VAF, %
S1	1.95	–	0.16	13.93	0.16	84.36
D1	0.25	1.33	0.23	11.33	0.18	86.03

IV.D. Modeling Behavior for Ramp-Following Tasks

IV.D.1. Pursuit/Precognitive Behavior Modeling

To investigate to what extent the model for Y_{p_t} proposed in Sec. II.C.2 can describe measured control inputs, the three parameters of the model (K_{p_t}, T_{I_t}, and τ_t) were fitted to the average time traces of u (see Fig. 10) for all conditions where a ramp target signal was present. Note that the full time traces of u were used to fit one set of parameters,

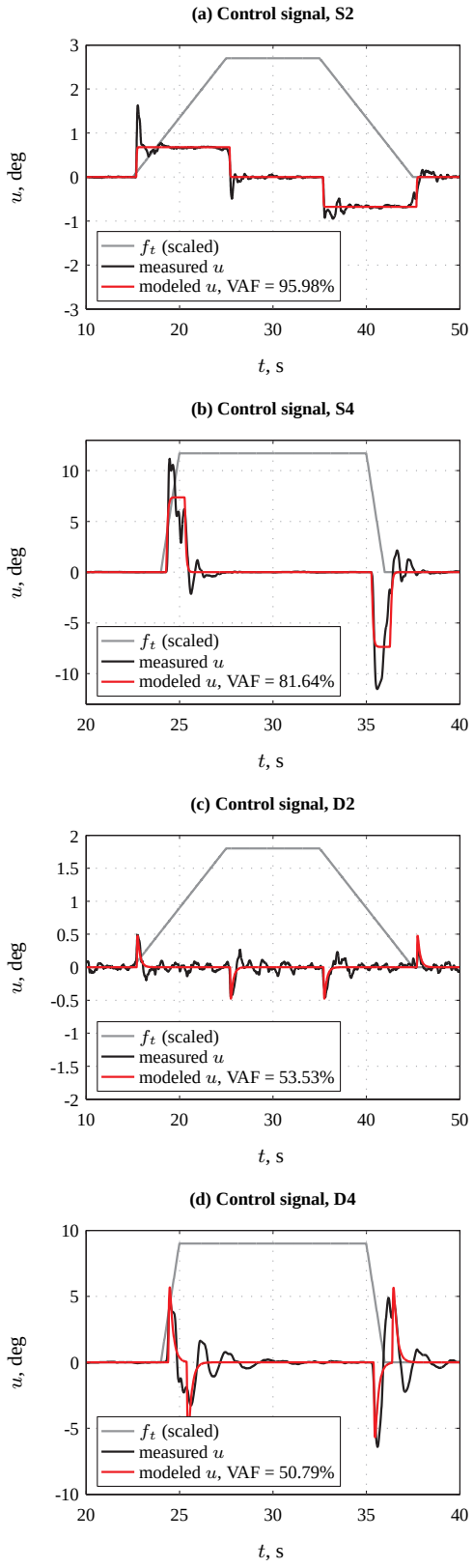

Figure 13. Feedforward control signal fits for pure ramp-following conditions (S2, S4, D2, and D4) for subject 1.

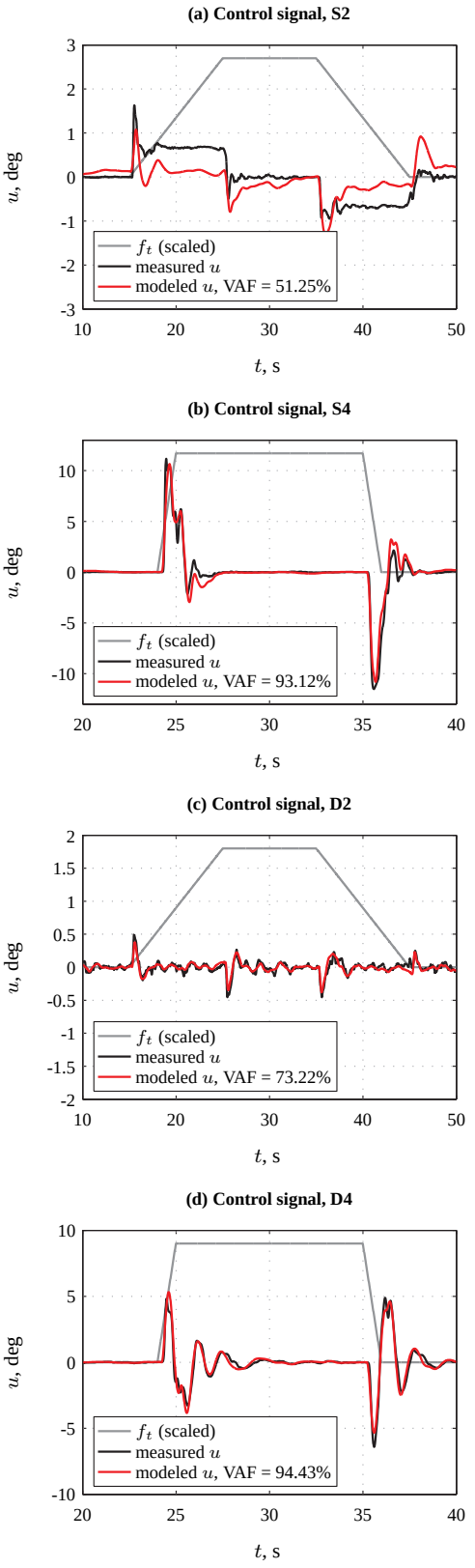

Figure 14. Compensatory control signal fits for pure ramp-following conditions (S2, S4, D2, and D4) for subject 1.

yielding parameter estimates based on control inputs for all four ramp-like changes in reference attitude occurring in the target signal (see Fig. 3). Fig. 13 depicts typical results of fitting the model of Eq. (4) to measurements of u for all ramp-tracking conditions where the disturbance signal was not present, that is, S2, S4, D2, and D4. The results shown in Fig. 13 were obtained for subject 1, but highly similar results were obtained for all other participants.

Note from Fig. 13 that for all four pure ramp-following conditions, the model of Eq. (4) is able to capture the initial control input given after a ramp in the target signal. As for instance visible in Fig. 13(b) and (d), the identification of the proposed model also appears to yield good estimates of the delay in the control response as defined in Fig. 5. Fig. 13, however, also illustrates that the model for Y_{p_t} is not capable of explaining all measured control inputs. For all conditions, the measured time traces of u show some overshoots and additional oscillatory inputs compared to the modeled control signals. In addition, as illustrated best by Fig. 13(c), even in the absence of f_d the unstable double integrator controlled element dynamics required significant (compensatory) control inputs for stabilization, also during periods where no ramp signal was to be followed. As will be discussed in more detail in Sec. IV.D.2, these additional control inputs can all be captured with the compensatory model (Eq. (2)), suggesting that subjects indeed performed compensatory control in addition to feedforward operations on f_t, as proposed in Fig. 6.

Fig. 15 depicts the mean estimated parameters of the model of Eq. (4) for all experimental conditions. Note that for the control tasks with only the quasi-random disturbance signal no target signal was present, and hence no estimates of the dynamics of Y_{p_t} were made. As in Fig. 11, the depicted variance bars indicate the 95% confidence intervals, corrected for between-subject variability.

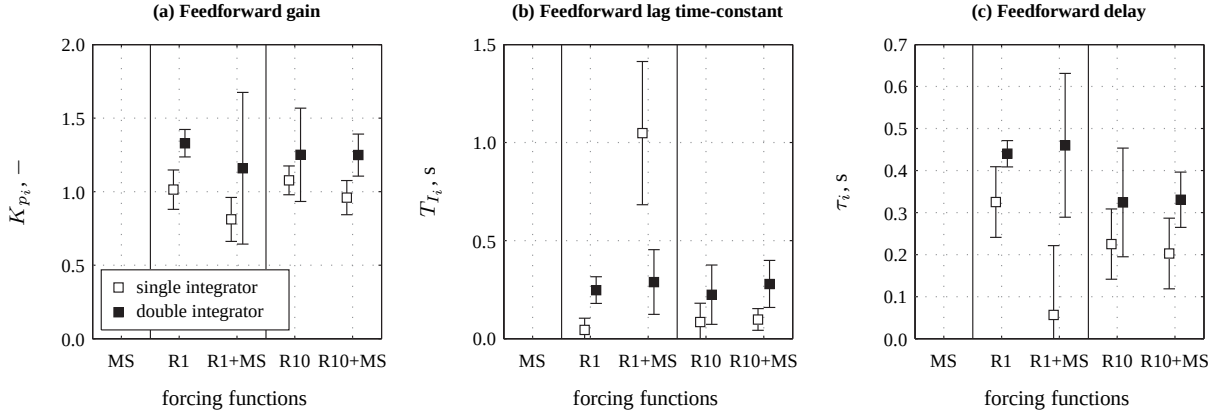

Figure 15. Average identified parameters of the pursuit/precognitive model of Eq. (4).

The first thing to note from Fig. 15 is the remarkable consistency, given a small number of exceptions, of the estimated parameters over the different conditions. In addition, note that on average the values of all three parameters are found to be markedly higher for the double integrator than for the single integrator dynamics. For the single integrator, the estimated feedforward gains K_{p_t} are found to be close to the theoretically optimal value of 1 ($Y_{p_t}Y_c \approx 1$), see Fig. 15(a). Notable is the fact that for the double integrator, this gain is found to be consistently higher than 1. Fig. 15(b) and (c) further indicate significantly more phase lag (higher T_{I_t}) and slightly more delay in Y_{p_t} (higher τ_t) for the double integrator dynamics.

Finally, Fig. 15 shows different estimated parameter values and significantly more spread in the results obtained for the conditions where the R1 ramp signal and the disturbance signal were both present (conditions S3 and D3). This can be explained by considering the control signal time traces depicted in Fig. 10(h). By comparing these measurements with the control input that would be modeled by Y_{p_t} (Fig. 13(a)), it is clear that the compensatory control inputs dominate those that would result from the feedforward, making identification of the model of Eq. (4) difficult.

IV.D.2. Compensatory Behavior Modeling

The compensatory model described in Sec. II.C.1 was fitted to the same averaged data as the model for Y_{p_t} using the time-domain maximum likelihood estimation procedure detailed in Ref. 21. Fig. 14 depicts the resulting modeled control signals for the same four conditions shown in Fig. 13. Note that these four conditions are those without the quasi-random disturbance signal, which theoretically would require the least compensatory control inputs.

Fig. 14(a) illustrates that for condition S2, the control inputs given to follow the R1 target signal can not be explained by the compensatory control model. The reason for that is the fact that, except for small errors due to the time between the occurrence of a ramp and the first control input, ramp tracking errors are negligible (see also

Fig. 10(e)). Note, however, by comparing Figures Fig. 13(a) and Fig. 14(a), that the compensatory model can fit the overshoots and slight oscillations present in the measured time traces of u that the model for Y_{p_t} misses.

Surprisingly, the model time traces depicted of the remaining three conditions in Fig. 14 reveal that the complete measured control signals – that is, both the initial and the final error-reducing compensatory control inputs, that is, phases II and III in Fig. 5 – are captured at reasonably high accuracy by the model of Eq. (2). This especially holds for the conditions with the steeper R10 ramps. The similarity of the error and control signals for condition S4 depicted in Fig. 10 explains this, as clearly enough tracking errors build up to fit the model for Y_{p_e} on. Note, however, that from these results it can not be concluded that pure compensatory control behavior was utilized for these conditions, as judging the results shown in Fig. 13 the total control input could still be the sum of both the Y_{p_e} and Y_{p_t} responses. Fig. 14, however, does show that the model of Eq. (2) is highly capable of capturing the oscillatory control inputs the model for Y_{p_t} fails to describe.

Fig. 16 depicts the mean estimated values of three of the parameters of the compensatory model of Eq. (2) – the proportional gain K_{p_e}, the lead time-constant T_{L_e}, and the time delay τ_e – for all experimental conditions. Again, the depicted variance bars indicate the 95% confidence intervals, corrected for between-subject variability.

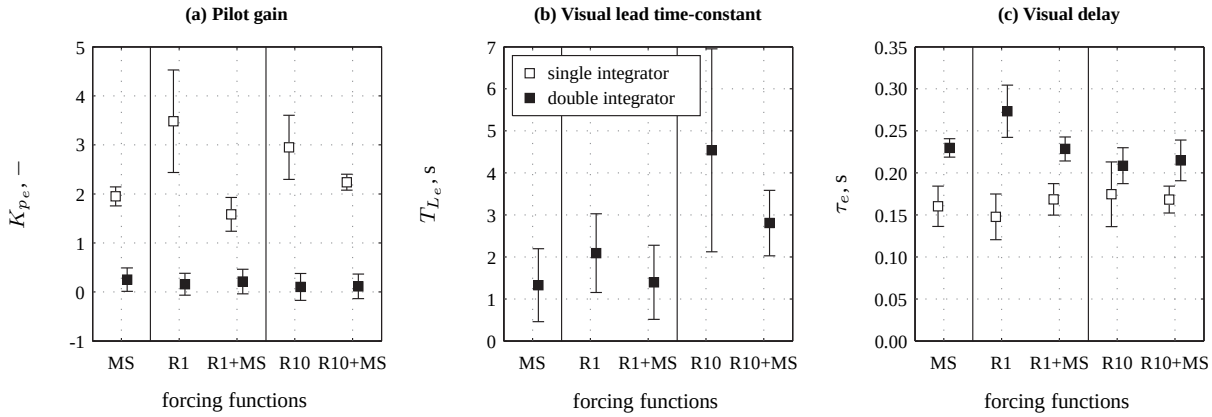

Figure 16. Average identified parameters of the compensatory model of Eq. (2).

Fig. 16 shows consistent estimates of K_{p_e}, T_{L_e}, and τ_e for all conditions where the disturbance signal was present. For the conditions with only ramp target signals, where less compensatory behavior would be expected, estimated parameter values clearly deviate from those of the pure compensatory conditions (MS) and tend to show more spread, indicating that only the model of Eq. (2) is not capable of consistently describing the measured data. The only very small differences observed between the compensatory model parameter estimates for the MS and R1+MS conditions for both controlled elements, however, do suggest dominant compensatory control behavior for conditions S3 and D3. Note that this corresponds well with the conclusions drawn from the estimated parameters of the pursuit/precognitive model of Eq. (4) presented in Fig. 15.

IV.D.3. Comparison of Model Variance Accounted For

The time traces for the model fits obtained for conditions S2, S4, D2, and D4 depicted in Figures 14 and 13 already indicate how well both models considered in this paper describe the measured control signals. Further qualitative evaluation of the goodness-of-fit of both models has been performed using the model variance accounted for as defined by Eq. (7). Fig. 17 depicts the average VAF for each conditions for both the pursuit/precognitive and compensatory models of Eq. (4) and (2), respectively.

Fig. 17(a) shows that, as expected, the VAFs of the pursuit/precognitive model are highest for the conditions with only ramp target signals. For the conditions where more compensatory control inputs are observed (see Fig. 10), clearly degraded VAFs are found. Similarly, note the marked offset in average VAF (but highly similar effect of the applied variation in forcing function signals) between the data for single and double integrator dynamics. As for instance illustrated by Fig. 13(c), this is caused by the additional compensatory effort required for stabilizing the unstable double integrator dynamics.

The compensatory model VAFs depicted in Fig. 17(b) show on average higher values than depicted in Fig. 17(a) for all conditions except S2 and D2 (R1). This is most likely caused by the difference in nature of both models: the compensatory model is able to provide a good fit over the full measurement time, while the feedforward model only provides a model fit around the ramps in the reference signal. Furthermore, note that the compensatory model is able to

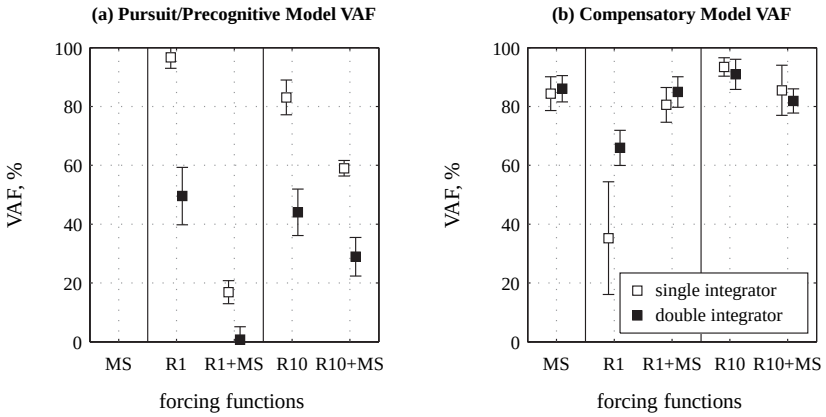

Figure 17. Comparison of goodness-of-fit in terms of model VAF for pursuit/precognitive and compensatory modeling of pilot control.

describe the data for all conditions where the disturbance signal is present with a VAF of over 80%. Severely degraded VAFs are observed for the conditions with only the R1 ramp signal, in line with the discussion of the fit shown in Fig. 14(a). The extremely high VAFs found for conditions S4 and D4 (R10) also correspond to the good fits obtained for this condition (see Fig. 14) and are also caused by the reduced variance in the measured control signals due to the absence of the disturbance signal.

V. Discussion

This paper investigated the modeling of human dynamics in control tasks where predictable target forcing function signals, consisting of multiple ramp-like changes in reference attitude, are tracked using a pursuit display. In addition, the effects of the presence of an additional quasi-random disturbance signal on the adopted control strategy were evaluated.

Based on the SOP theory described by McRuer et al.,[1] it would be expected that the use of predictable forcing function signals would yield some precognitive control inputs. In addition, the use of a pursuit display would allow for a pursuit tracking strategy. The work of Wasicko et al.,[12] Allen and McRuer,[16] and McRuer and Krendel,[10] indicate that both pursuit and precognitive control can be modeled with a similar model of human behavior, which combines compensatory (error reducing) control with feedforward operations on the predictable reference signal. This paper evaluated the modeling of both these contributions to the total control behavior separately, thereby allowing for comparison of their relative importance for the different experimental conditions.

For identification of the feedforward dynamics, a model was proposed that yielded a human feedforward response proportional to the inverse of the controlled element dynamics, filtered by a pure first-order lag and a pure time delay. Though leaving room for extension, this model was found to be capable of identifying the time delay associated with the feedforward control inputs. In addition, for both single and double integrator controlled element dynamics, the initial model response to the ramps in the forcing function signals were found to correspond well with measured control inputs.

Measurement of pure compensatory pilot dynamics for both single and double integrator controlled element dynamics during tracking with the quasi-random disturbance only yielded estimates of the compensatory model parameters that are highly consistent with previous research.[2] In addition, for the data from the tasks where the same disturbance signal was applied in addition to a ramp target signal, highly similar compensatory model estimates were obtained, suggesting nearly constant compensatory human operator dynamics. If compensatory control dynamics indeed stay constant when pursuit or precognitive control strategies are applied as proposed by McRuer and Krendel[10] and Wasicko et al.,[12] the model parameters obtained for the pure compensatory conditions (as listed in Table 4) should to some extent be capable of describing the compensatory control adopted in the conditions where ramp target signals were present in addition to the disturbance f_d. Such a generalization of the results presented in this paper is deemed important future work.

Concluding, based on the SOP theory and the experimental results described in this paper, a dual-mode model of human behavior that includes both compensatory and feedforward operations seems appropriate for modeling measured control behavior in control tasks with predictable forcing function signals. The results shown in this paper suggest that for low-steepness ramp signals combined with a quasi-random disturbance pure compensatory model-

ing might, however, still be acceptable. Table 5 summarizes the required model structure for the different conditions evaluated in the experiment described in this paper.

Table 5. Appropriate manual control model structure for all experimental conditions.

Condition	Forcing functions	Required model
S1,D1	MS	Y_{p_e}
S2,D2	R1	$Y_{p_e} + Y_{p_t}$
S3,D3	R1+MS	$Y_{p_e}(+Y_{p_t})$
S4,D4	R10	$Y_{p_e} + Y_{p_t}$
S5,D5	R10+MS	$Y_{p_e} + Y_{p_t}$

This paper has not yet evaluated a model of human behavior that incorporated both the compensatory and feedforward elements as depicted in Fig. 6. Evaluation of such a combined model for the selected conditions listed in Table 5 is expected to be performed in the coming months. In addition, the extent to which the modeling of ramp-following behavior described in this paper also applies manual control in the presence of physical motion feedback will be evaluated in future human-in-the-loop experiments.

VI. Conclusions

The modeling of human manual control behavior in control tasks where predictable forcing function signals, such as signals consisting of multiple ramp-like changes in target attitude, are applied could require models of human behavior that account for both compensatory behavior and feedforward operations on the reference signal. This paper described the results of an experiment and corresponding modeling effort aimed at revealing if such dual-mode models are indeed required for modeling the tracking of ramp signals with different ramp steepnesses. In addition, the impact on the modeling of human behavior for control tasks where an additional quasi-random disturbance forcing function is applied, which can only be attenuated through compensatory control, was also evaluated. The proposed model for capturing open-loop feedforward control was found to accurately capture the initial control inputs resulting from the predictable forcing function signals. From measured control signal time traces, the need for modeling additional compensatory control was, however, found to be evident for all evaluated conditions. Compensatory behavior even appears to be dominant for the control tasks that combine low-steepness ramp signals with a quasi-random disturbance.

Acknowledgments

This research was supported by the Dutch Technology Foundation (STW), the applied science division of The Netherlands Organization for Scientific Research (NWO), and the technology program of the Ministry of Economic Affairs.

References

[1]McRuer, D. T., Hofmann, L. G., Jex, H. R., Moore, G. P., and Phatak, A. V., "New Approaches to Human-Pilot/Vehicle Dynamic Analysis," Tech. Rep. AFFDL-TR-67-150, 1968.

[2]McRuer, D. T., Graham, D., Krendel, E. S., and Reisener Jr., W., "Human Pilot Dynamics in Compensatory Systems. Theory, Models and Experiments with Controlled Element and Forcing Function Variations," AFFDL-TR 65-15, Air Force Flight Dynamics Laboratory, Wright-Patterson AFB (OH), August 1965.

[3]Jex, H. R., Magdaleno, R. E., and Junker, A. M., "Roll Tracking Effects of G-Vector Tilt and Various Types of Motion Washout," *Fourteenth Annual Conference on Manual Control*, 1978, pp. 463–502.

[4]Hosman, R. J. A. W., *Pilot's Perception and Control of Aircraft Motions*, Ph.D. thesis, Delft University of Technology, Faculty of Aerospace Engineering, 1996.

[5]Zaal, P. M. T., Pool, D. M., Mulder, M., and Van Paassen, M. M., "Multimodal Pilot Control Behavior in Combined Target-Following Disturbance-Rejection Tasks," *Journal of Guidance, Control and Dynamics*, Vol. 32, No. 5, 2009, pp. 1418–1428.

[6]Stapleford, R. L., Peters, R. A., and Alex, F. R., "Experiments and a Model for Pilot Dynamics with Visual and Motion Inputs," Tech. Rep. NASA CR-1325, Systems Technology, Inc., Hawthorne (CA), 1969.

[7]Zaal, P. M. T., Pool, D. M., Mulder, M., and Van Paassen, M. M., "New Types of Target Inputs for Multi-Modal Pilot Model Identification," *Proceedings of the AIAA Modeling and Simulation Technologies Conference and Exhibit, Honolulu (HI)*, No. AIAA-2008-7106, 2008.

[8]Pool, D. M., Zaal, P. M. T., Van Paassen, M. M., and Mulder, M., "Identification of Roll Attitude Control Behavior During Turn Maneuvers," *Proceedings of the AIAA Modeling and Simulation Technologies Conference and Exhibit, Chicago (IL)*, No. AIAA-2009-6029, 2009.

[9]Pool, D. M., Zaal, P. M. T., Mulder, M., and Van Paassen, M. M., "Identification of Multimodal Pilot Models Using Ramp Target and Multisine Disturbance Signals," *Journal of Guidance, Control, and Dynamics*, Accepted for publication.

[10]McRuer, D. T. and Krendel, E. S., "Mathematical Models of Human Pilot Behavior," AGARD-AG 188, Advisory Group for Aerospace Research and Development, January 1974.

[11]McRuer, D. T., "Human Dynamics in Man-Machine Systems," *Automatica*, Vol. 16, 1980, pp. 237–253.

[12]Wasicko, R. J., McRuer, D. T., and Magdaleno, R. E., "Human Pilot Dynamic Response in Single-Loop Systems with Compensatory and Pursuit Displays," AFFDL-TR 66-137, Wright-Patterson AFB(OH): Air Force Flight Dynamics Laboratory, December 1966.

[13]Hess, R. A., "Pursuit Tracking and Higher Levels of Skill Development in the Human Pilot," *IEEE Transactions on Systems, Man, and Cybernetics*, Vol. SMC-11, No. 4, 1981, pp. 262–273.

[14]Reid, L. D., "An Investigation into Pursuit Tracking in the Presence of a Disturbance Signal," *Proceedings of the Fifth Annual NASA University Conference on Manual Control*, No. NASA SP-215, 1970, pp. 129–169.

[15]Zaal, P. M. T., Pool, D. M., Mulder, M., Van Paassen, M. M., and Mulder, J. A., "Identification of Multimodal Pilot Control Behavior in Real Flight," *Journal of Guidance, Control and Dynamics*, Accepted for publication.

[16]Allen, R. W. and McRuer, D. T., "The Man/Machine Control Interface – Pursuit Control," *Automatica*, Vol. 15, No. 6, 1979, pp. 683–686.

[17]Damveld, H. J., Abbink, D. A., Mulder, M., Van Paassen, M. M., Van der Helm, F. C. T., and Hosman, R. J. A. W., "Measuring the Contribution of the Neuromuscular System during a Pitch Control Task," *Proceedings of the AIAA Modeling and Simulation Technologies Conference and Exhibit, Chicago (IL)*, No. AIAA-2009-5824, 2009.

[18]Stroosma, O., Van Paassen, M. M., Mulder, M., and Postema, F. N., "Measuring Time Delays in Simulator Displays," *Proceedings of the AIAA Modelling and Simulation Technologies Conference and Exhibit, Hilton Head (SC)*, No. AIAA-2007-6562, 2007.

[19]Zaal, P. M. T., Pool, D. M., De Bruin, J., Mulder, M., and Van Paassen, M. M., "Use of Pitch and Heave Motion Cues in a Pitch Control Task," *Journal of Guidance, Control and Dynamics*, Vol. 32, No. 2, 2009, pp. 366–377.

[20]Damveld, H. J., *A Cybernetic Approach to Assess the Longitudinal Handling Qualities of Aeroelastic Aircraft*, Ph.D. thesis, Delft University of Technology, Faculty of Aerospace Engineering, May 2009.

[21]Zaal, P. M. T., Pool, D. M., Chu, Q. P., Van Paassen, M. M., Mulder, M., and Mulder, J. A., "Modeling Human Multimodal Perception and Control Using Genetic Maximum Likelihood Estimation," *Journal of Guidance, Control and Dynamics*, Vol. 32, No. 4, 2009, pp. 1089–1099.